Physical and electrochemical chattels of phosphonium ionic liquid-based solid and gel-polymer electrolyte for lithium secondary batteries

R. Muthupradeepa[1,2], M. Sivakumar[1,*] , R. Subadevi[1], V. Suriyanarayanan[3], M. Ramachandran[1,4], P. Rajkumar[1], and R. Yuvakkumar[1]

[1] #120, Energy Materials Lab, Department of Physics, Alagappa University, Science Block, Karaikudi, Tamil Nadu 630003, India
[2] Sree Sastha Institute of Engineering and Technology, Chennai, Tamil Nadu 600123, India
[3] Electro-Organic Division, Central Electrochemical Research Institute, Karaikudi, Tamil Nadu 630 006, India
[4] Department of Physics, Arumugam Pillai Seethai Ammal College, Tiruppathur, Tamil Nadu 630211, India

ABSTRACT

In this work, a methodical study on the influence of ionic conductivity on polymer electrolyte with different weight percentages of ionic liquid and plasticizers had been investigated in detail. Solution casting method has been employed for preparing polymer electrolyte (PE) blend having poly(vinylidenefluoride-*co*-hexafluoropropylene) P(VdF-*co*-HFP) as polymer, trihexyltetradecylphosphonium bis(trifluoromethylsulfonyl) amide $[P_{14,6,6,6}][Tf_2N]$ as ionic liquid and ethylene carbonate (EC) as well as propylene carbonate (PC) in 1:1 ratio as plasticizers. The polymer electrolyte has been found out stable up to 450 °C, as measured from Thermal gravimetric analysis (TGA). Impedance spectral analysis reveals that the ionic conductivity of SPEs is 3.209×10^{-6} S/cm at 303 K with 25 wt% of ionic liquid. The addition of plasticizers (EC + PC (60 wt%)) results in two orders of magnitude of higher ionic conductivity (3.40×10^{-4} S/cm at 303 K), than that of SPEs. X-ray diffraction (XRD), Fourier transform infrared spectroscopy (FTIR) and scanning electron microscope (SEM) are performed to study the physico-chemical characteristics of polymer electrolytes. Electrochemical stability, potential window and discharge characteristics of the coin cell containing the electrolytes and $LiFePO_4$ electrode were investigated using linear and cyclic voltammetry.

Address correspondence to E-mail: sivakumarm@alagappauniversity.ac.in; susiva73@yahoo.co.in

 Springer

1 Introduction

The lithium batteries are the utmost choice for high energy consuming devices because of their properties which relate to their high working voltage, high energy density, long cycle life, better mechanical property and size effective [1–3]. Electrolytes with electro active properties such as ionic conductivity, electro chemical window, cyclic shall play a vital role in electrochemical devices. Electrolytes belonging to polymer electrolytes have higher conductivity, high thermal and mechanical stability, wide electro chemical window and so on [4–6]. Whereas Organic electrolytes as well as solid polymer electrolytes fails in these properties such as flammability, volatility, lithium dendrites, leakage, hazards to nature and poor contact between electrodes, [7]. On the other hand, ionic liquid incorporated polymer electrolyte matrix provides mechanical support, whereas ionic liquid itself gives the anion and cation for ionic conductivity [8]. However, selection of suitable polymer host and an ionic liquid is very important. High chemical stability and strong electron withdrawing functional groups are the most desirable property of a polymer. One of the polymer widely investigated is poly(vinylidenefluoride-*co*-hexafluoropropylene) P(VdF-*co*-HFP) for its high dielectric constant ($\varepsilon = 8.4$) and facilitation of high number of charge carriers. The crystallinity present in the semi-crystalline polymer retains adequate mechanical stability to activate as a separator for the electrodes, while the amorphous phase provides sufficient conducting nature [9–12]. On the other hand, P(VdF-*co*-HFP) retains more electrolyte solutions due to its low crystallinity associated with excellent chemical resistance, mechanical and thermal properties, etc., [13, 14].

Molten salts have the appearance of liquid at room temperature are called as ionic liquid. Ionic liquids have received great attention from researchers due to their potential applications with excellent physical and chemical properties. Ionic liquids have very interesting property such as low vapor pressure, non-volatility, high thermal stability, high electro chemical window [15, 16]. With the prevailing properties, ionic liquids are considered as one of the best choice of materials for lithium battery fabrication in modern world technology [17, 18]. Organic or inorganic anions and organic cations which are poorly bonded are known as ionic liquids. This asymmetric structure makes them hard to crystallize; hence they have liquid nature with wide temperature range [19]. In the first generation of ionic liquids, attention is being paid in imidazolium-based cation for its high conductivity and low viscosity. But in the view of its low electrochemical window due to its acidic proton, it has limited applications. Phosphonium ionic liquids have particular strong property of negligible vapor pressure, high thermal capacity, and wide liquid range [20]. Phosphonium architecture-based ionic liquids have particular property compared to ammonium, pyridinium and imidazolium cationic counter parts, as it does not have acidic proton [21, 22]. Phosphonium cation has four different substituents and good chance to bonding with large number of anions [23]. Phosphonium-based ionic liquids exhibit high thermal stability and high electrochemical stability window. Due to its high viscosity (295.91 mPa s at 25 °C), it restricts the ionic mobility and offers low ionic conductivity (0.89 mS/cm) compared to other ionic liquids. Columbic interaction between anion and cation results in high viscosity and highly delocalized cation compose the ionic liquid as liquid at room temperature [24]. Ionic liquids with Tf_2N exhibit low viscosity and wide electrochemical stability due to the delocalized charge in Tf_2N, which leads to flexible structure and weak interaction with other charges [25].

Ethylene and propylene carbonate (EC and PC) plasticizer in 1:1 ratio was added to the IL to improve its poor ionic conductivity caused by high viscosity of phosphonium cation. The gel polymer electrolyte formed with organic carbonate provides necessary viscosity to the cationic phosphonium leads to swamped viscosity. Organic carbonates (EC and PC) dissociate the columbic interaction in ionic liquids because of their high dielectric constant such as $\varepsilon = 89.78$ at 40 °C and 64.93 at 25 °C, respectively [26].

In this framework, solid and gel polymer electrolytes (SPEs and GPE) were prepared using solution casting method; P(VdF-*co*-HFP) polymer has been modified using of trihexyltetradecylphosphonium bis(trifluoromethylsulfonyl) amide $[P_{14,6,6,6}]$ $[Tf_2N]$ ionic liquid. For energy storage applications, the optimized electrolyte has been elucidated respectively from different ratios of polymer to ionic liquid such as (95–5 wt%, 90–10 wt%, 85–15 wt%, 80–20 wt% and 75–25 wt%). The GPE has been prepared by adding EC and PC in SPE. The maximum

conductivity and the physical as well as electrochemical properties of the polymer matrix have been found out from their optimum ratio for lithium battery application. The effect of ionic liquid and plasticizer in PE has been studied by subjecting them for different characterizations. The physical property has been studied using X-ray diffraction measurements (XRD), Fourier transform infrared spectrometer (FTIR), thermo gravimetric and differential thermal analysis (TG/DTA), and scanning electron microscopy (SEM), while the electrochemical properties have been analyzed using AC impedance, linear sweep voltammetry (LSV), cyclic voltammetry (CV) and charge- discharge (C/D) analyses.

2 Experimental

Poly(vinylidene fluoride-*co*-hexafluoropropylene) P(VdF-*co*-HFP) as polymer matrix, trihexyltetradecylphosphonium bis(trifluoromethylsulfonyl) amide [$P_{14,6,6,6}$] [Tf_2N] ionic liquid, ethylene carbonate (Merck, India) and propylene carbonate are the basic chemicals used in this work. Solution casting method has been employed to prepare the polymer electrolytes in the ratios mentioned in Table 1. The polymer PVdF-*co*-HFP and ionic liquid [$P_{14,6,6,6}$][Tf_2N] both were received from Sigma Aldrich USA and used without further purification. Tetrahydrofuran (THF) was used as a solvent to dissolve the polymer and to prepare the polymer matrix. Organic solvents were purchased from SRL India and used as received. As mentioned in Table 1, the calculated amount of polymer was dried in vacuum under 1×10^{-3} Torr pressure in a temperature-controlled vacuum oven at 100 °C for 10 h. The

moisture and impurity present in the polymer was removed by the vacuum heating process. An efficient amount of solvent THF was poured in the polymer to make polymer solution by stirring. The calculated amount of ionic liquid or ionic liquid with EC and PC was added to the above polymer solution, which was stirred continuously to obtain homogeneity. A flat bottom petri plate has been used to cast the mixture of polymer ionic liquid solution to obtain thin electrolyte film. Finally, freestanding films were dried at 60 °C under vacuum for 5 h.

The PANalytical X'Pert PRO powder X-ray diffractometer using Cu-Kα radiation as source and operated at 40 kV had been used to study the variation of crystalline nature as the function of ionic liquid ratio. The FTIR Thermo Nicolet 380 spectrometer was used to study the interactions of different fundamental vibrational groups in the range of 4000 to 400 cm^{-1}. Thermal analysis was performed using STA 409 PL Luxxat a heat rate of 10 °C/min within the temperature range from room temperature to 900 °C under Nitrogen atmosphere. The surface nature has been studied with SEM Model JEOL-JSM-6500F at an accelerating voltage of 5 kV and 15 kV after sputtering platinum over the samples.

AC impedance technique has been performed to find out the conductivity of the ionic liquid polymer electrolytes sandwiched between stainless steel (SS) blocking electrodes. A computer-controlled micro Autolab III Potentiostat/Galvanostat with frequency range from 1 Hz to 500 kHz with a signal amplitude of 10 mV, were used to study the conducting behavior at different temperature ranging from 303 to 353 K. The bulk resistance obtained from the complex impedance plot has been employed for ionic conductivity calculation. For other electrochemical

Table 1 The calculated weight percentage, ionic conductivity and activation energy values of solid and gel polymer electrolytes PVdF-*co*-HFP, [P14,6,6,6][Tf$_2$N], EC + PC

PVdF-*co*-HFP + [P14,6,6,6][Tf$_2$N] (wt%)	EC + PC (wt%)	Sample code/ temperature	Conductivity $\times 10^{-6}$ S/cm						E_a values (eV)
			303 K	313 K	323 K	333 K	343 K	353 K	
95 + 5	0	K1	0.0470	0.0581	0.1303	0.1740	0.1942	0.2525	0.429
90 + 10	0	K2	0.0974	0.2429	0.4507	0.7026	1.1541	2.4014	0.390
85 + 15	0	K3	1.1506	1.5145	2.4737	4.4781	12.143	22.463	0.334
80 + 20	0	K4	1.7375	2.2175	3.6032	6.9046	25.502	40.345	0.321
75 + 25	0	K5	3.2090	4.1876	6.8012	19.249	31.483	58.813	0.305
75 + 25	60	K6	340.23	388.32	484.87	676.36	1205.36	1579.76	0.197

analysis, coin cells have been fabricated for high ionic conducting electrolyte sample. Li has been used as reference and counter electrode. Working electrode has been fabricated with 80:10:10 ratios of LiFePO$_4$:-PVdF:Super P carbon. The above combination was prepared as slurry using NMP solvent and coated on Alumina foil and then dried at 80 °C for 6 h. Then the coil cells (CR 2032) have been fabricated for electrochemical characterization. The electrochemical studies were carried out using Autolab electrochemical workstation (GPES, PGSTAT 302N).

3 Results and discussion

3.1 X-ray diffraction

Figure 1 shows X- ray diffraction pattern of pure P(VdF-co-HFP) and mixed SPEs and GPE in the ratio as mentioned in Table 1. It is clearly visible that the pure polymer P(VdF-co-HFP) has semi-crystalline nature, where the crystalline peaks with 2θ angle at 18.44°, 20.13° and 39.04° reflect the α phase of crystalline plane [27]. The representation of these peaks makes the atoms to arrange in lattice and remaining amorphous nature is responsible for ionic conductivity [28]. However, in SPEs and GPE, the appeared peaks corresponding to P(VdF-co-HFP) are wider and reduce the crystalline domains and try to form an
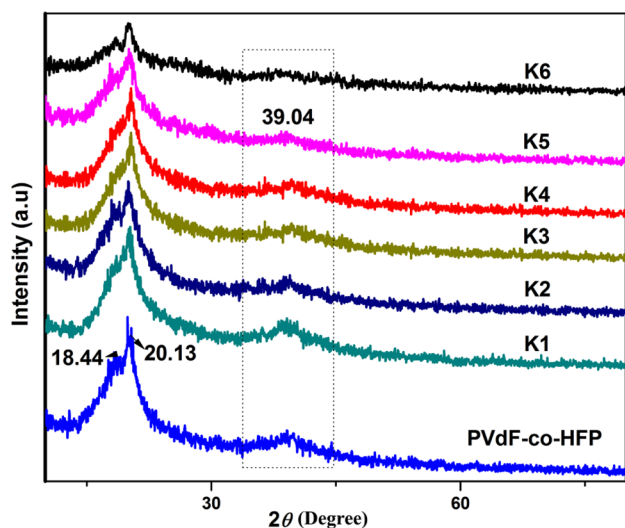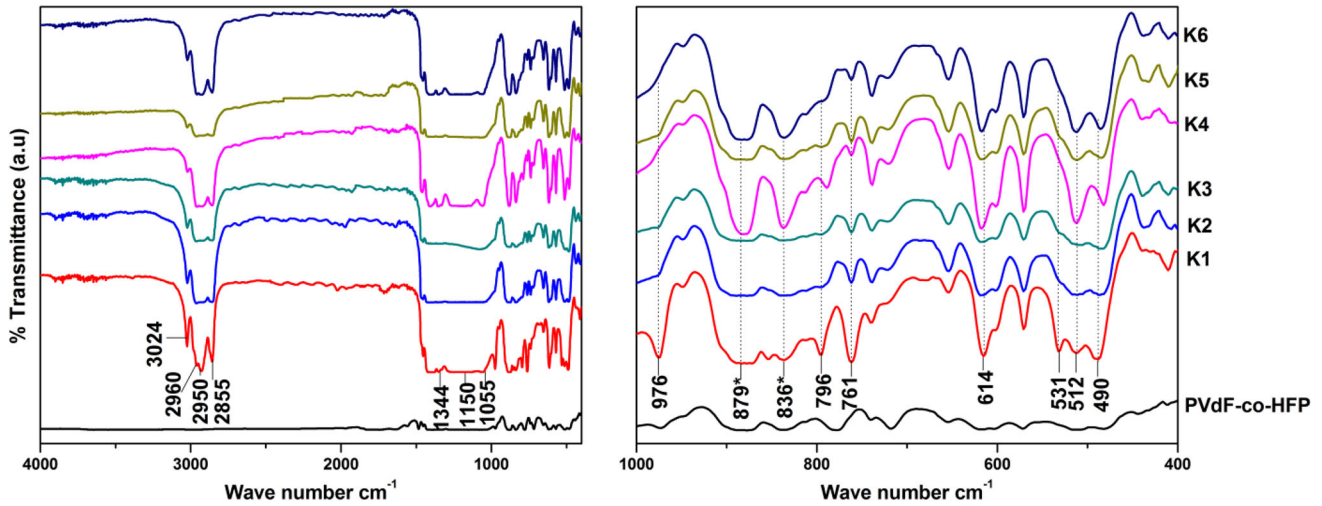

Fig. 1 X-ray diffraction pattern of pure P(VdF-co-HFP), different SPE K1-(95:5), K2- (90:10), K3- (85:15), K4- (80:20), K5-(75:25) of P(VdF-co-HFP) + [P$_{14,6,6,6}$][Tf$_2$N] and GPE K6-PVdF-co-HFP + [P$_{14,6,6,6}$][Tf$_2$N] (75:25) + EC + PC (60) wt%

amorphous system. Here, intensity of the resultant peaks for P(VdF-co-HFP) polymer matrix blended with [P$_{14,6,6,6}$][Tf$_2$N] as well as [P$_{14,6,6,6}$][Tf$_2$N] + EC + PC decreases drastically, which shows weak peaks with wide nature in all cases. From the patterns, it is noted that intensities of the peak decreases upon increasing IL content. When compared to the SPEs, the diffraction pattern of electrolyte with EC + PC shows nearly a flat pattern. This peak is representing high amorphous nature, which is responsible for high ionic conductivity.

3.2 FTIR analysis

Figure 2 represents the FTIR spectra in the region of 4000 to 400 cm^{-1} of pure P(VdF-co-HFP) and IL imported PEs. The wavenumber between 1000 and 400 cm^{-1} have been magnified to view the spectrum more clearly. A crystalline phase of P(VdF-co-HFP) obtained at 490 cm^{-1}, 512 cm^{-1}, 531 cm^{-1}, 614 cm^{-1}, 761 cm^{-1}, 796 cm^{-1}, 976 cm^{-1} represent the presence of the P(VdF-co-HFP) in the complex system. The vibrations at 490 cm^{-1} and 512 cm^{-1} represent the bending and wagging modes of CF$_2$ group, whereas the wave number at 531 cm^{-1} and 976 cm^{-1} ascribe to nonpolar TGTG trans gauche conformation [29]. The CF$_2$ bending and CCC skeletal vibration are noted from the wave number at 614 cm^{-1}. The vibrational peak at 796 cm^{-1} stands for CF$_3$ stretching for polymer. Here, peaks 839 cm^{-1} and 879 cm^{-1} represent the β amorphous phase of polymer (represented by * in Fig. 2), where, the mixed mode of CH$_2$ rocking and CF$_2$ asymmetric stretching appears at 839 cm^{-1} and 879 cm^{-1} corresponding to CF$_2$ and CC symmetric stretching vibrations. The appearance of peaks at 2960 cm^{-1} and 3024 cm^{-1} represent the C-H stretching polymer [11]. The Tf$_2$N anion has been confirmed from the obtained peaks at 1348 cm^{-1}, 1196 cm^{-1}, 1136 cm^{-1} and 1055 cm^{-1}, and the peaks in the complexes are shifted to 1344 cm^{-1}, 1055 cm^{-1}. The remaining peaks combine together and form may be due to more thickness of the film a single band. A band existing at 1150 cm^{-1} represent the P = O group in [P$_{14,6,6,6}$] of IL. The appearance of peaks at 2855 cm^{-1} and 2950 cm^{-1} represent the CH$_2$ bonds of the aliphatic chains presented in phosphonium cation [30]. The shifting and disappearance of peaks confirms the formation of complexation between the polymer and ionic liquid. While increasing the ionic liquid content, most of the

Fig. 2 FTIR spectra of pure P(VdF-*co*-HFP), different SPE K1-(95:5), K2- (90:10), K3- (85:15), K4- (80:20), K5- (75:25) of P(VdF-*co*-HFP) + [P$_{14,6,6,6}$][Tf$_2$N] and GPE K6-PVDF-*co*-HFP + [P$_{14,6,6,6}$][Tf$_2$N] (75:25) + EC + PC (60) wt% system

crystalline peaks become weaker and amorphous peak becomes broader. This shows that the high content of ionic liquid tries to form an amorphous phase.

3.3 Ionic conductivity

The ionic conductivity values of the electrolytes have been estimated through AC impedance studies by observing real and imaginary parts for plotting CI plot. Figure 3a displays the complex impedance (CI) plot of P(VdF-*co*-HFP) polymer electrolyte with different [P$_{14,6,6,6}$][Tf$_2$N] contents and GPE at room temperature. It is noted that the CI plots of SPEs reflects the general of ionic solids with a typical semicircle and a spike behavior, whereas, only spike is appeared in GPE [30, 31]. The intercept of the semicircle or the spike with higher frequency in Z′ real axis gives the information about bulk resistance (R_b) of the polymer electrolyte [32, 33]. The conductivity values were calculated using the following equation:

$$\sigma = \frac{l}{AR_b} \qquad (1)$$

where σ is the ionic conductivity value, l is thickness of the electrolyte, A is the area of the film and R_b is the bulk resistance. It is observed that from Fig. 3a the size of semicircle portion of CI plot at room temperature decreases upon the addition of IL; at one stage, the semicircle has been disappeared. Also it is noted that the incorporation of the plasticizer causes a complete elimination of the semicircle [34]. The ionic conductivity values are proportional to [P$_{14,6,6,6}$][Tf$_2$N] content (Table 1). The higher content of [P$_{14,6,6,6}$][Tf$_2$N] suggests more amount of liquid electrolyte with maximum ionic conductivity of 3.209×10^{-6} S/cm at 303 K with 25 wt% of IL. These can be simply explained as follows: high content of [P$_{14,6,6,6}$][Tf$_2$N] in electrolyte has more number of free ions and these ions have very weak interaction with the polymer compared to the metallic salts [35]. These free ions found in polymer electrolyte have migrated easily through their free volume and results in higher conductivity. The addition of high amount of ionic liquid (beyond 25 wt%) produces higher conductivity among the polymer electrolyte studied. It is comparable with the earlier reports that the 100% of [P$_{14,6,6,6}$][Tf$_2$N] has ionic conductivity of the order of 8.9×10^{-4} S/cm at 303 K [24] and 1.34×10^{-4} S/cm at 303 K as reported by Battez et al. [30]. The major disadvantage with ionic liquid limits their use in industrial application due to its high cost. Because of this, the content of ionic liquid is restricted to 25% in SPEs. The concept of GPE has been introduced to reduce the viscosity of IL in polymer electrolytes. However, the plasticizer selection is made with EC + PC plasticizer with 60 wt%. The inclusion of plasticizer in SPE has found to increase the ionic conductivity up to two orders of magnitude. The prepared gel polymer electrolyte has ionic conductivity of 3.40×10^{-4} S/cm at 303 K. Hence, it is concluded that, the inclusion of plasticizer induces the conductivity in ILPE.
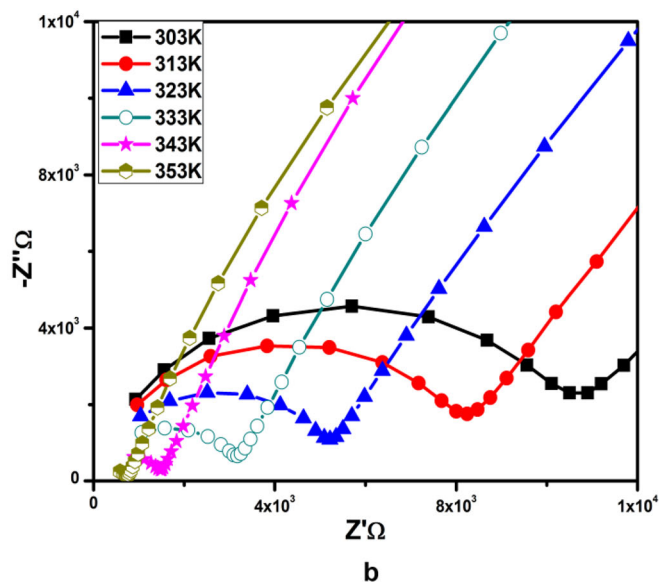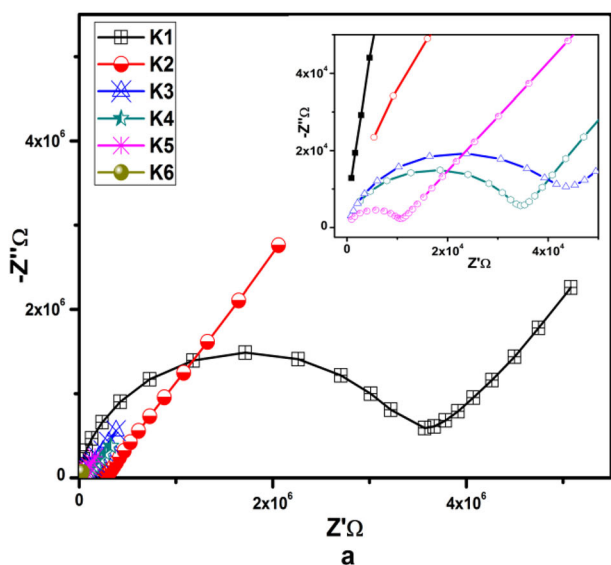
Fig. 3 **a** Complex impedance plot for SPE K1-(95:5), K2-(90:10), K3- (85:15), K4- (80:20), K5- (75:25) of P(VdF-*co*-HFP) + [P$_{14,6,6,6}$][Tf$_2$N] and GPE K6 P(VdF-*co*-HFP) + [P$_{14,6,6,6}$][Tf$_2$N] (75:25) + EC + PC (60) wt% in the SS/GPE/SS cell at room temperature, **b** Complex impedance plot of K5 P(VdF-*co*-HFP) + [P$_{14,6,6,6}$][Tf$_2$N] (75:25) at different temperatures

In order to understand ionic conducting behavior at different temperatures, the ionic conductivity of K1–K6 has been studied between 303 and 353 K and Fig. 3b shows the CI plot of K5 at various temperatures. In phosphonium-based ionic liquids, the higher viscosity with huge number of ions does not form a completely amorphous system leading to poor ionic conductivity, than sulphonium IL-based system.

The temperature-dependent ionic conductivity plot of all electrolytes in the variation of ionic conductivity values as a function of temperature has been plotted and shown in Fig. 4. The ion conducting behavior of the prepared electrolytes, (K1–K6) obeys the Arrhenius behavior and satisfies the Arrhenius relation given below:

$$\sigma = \sigma_0 \exp(E_a/kT) \tag{2}$$

where σ is the conductivity, σ_0 is the pre exponential factor, E_a activation energy, k is the Boltzmann constant and T is the absolute temperature. From the slope of the straight line, the activation energy values have been calculated and listed in Table 1. The activation energies of SPE (K5) and GPE (K6) with and without plasticizers are 0.305 eV and 0.197 eV, respectively. The maximum conducting sample in SPE category, it requires minimum activation energy. Still the requirement of energy is reduced upon adding plasticizer 60 wt%.
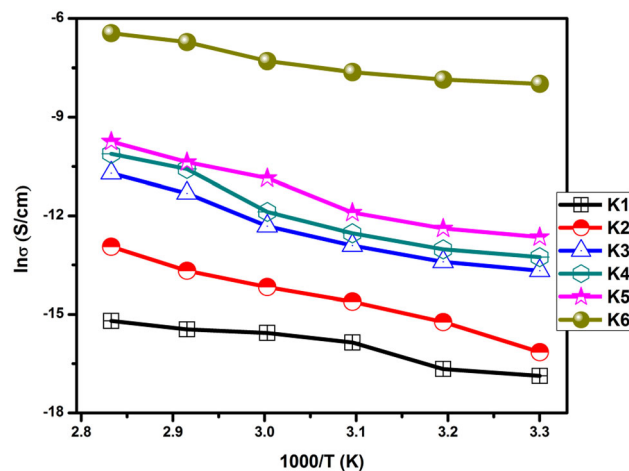
Fig. 4 Arrhenius plot of samples SPE K1-(95:5), K2- (90:10), K3- (85:15), K4- (80:20), K5- (75:25) of P(VdF-*co*-HFP) + [P$_{14,6,6,6}$][Tf$_2$N] and GPE K6 P(VdF-*co*-HFP) + [P$_{14,6,6,6}$][Tf$_2$N] (75:25) + EC + PC (60) wt% between the temperature 303 K to 353 K

The conductivity of 5 wt% of IL has lower value of conductivity, which is almost non-conducting due to the lesser number of charge carriers and due to the semi-crystalline nature of P(VdF-*co*-HFP). With the increase of the temperature, the polymer chains are more flexible and produce larger number of free volumes, which helps for easy ionic migration leading to higher ionic conductivity. The increase of

temperature also lowers the crystalline nature. At high ionic liquid and plasticizer content, the numbers of charge carriers are more and produce simply more pathways for cation and anions.

3.4 Scanning electron microscope (SEM) studies

The surface morphology of the prepared P(VdF-*co*-HFP) + [P$_{14,6,6,6}$][Tf$_2$N] electrolytes was studied using SEM. Figure 5 represents the surface structure of pure P(VdF-*co*-HFP) as well as P(VdF-*co*-HFP) + [P$_{14,6,6,6}$][Tf$_2$N] or P(VdF-*co*-HFP) + [P$_{14,6,6,6}$][Tf$_2$N] + EC + PC electrolytes with the magnification of 1 K. The pure P(VdF-*co*-HFP) electrolyte shows many spherical balls like structure and they are uniformly distributed though out the matrix. These balls are responsible for the crystalline nature of the polymer matrix [27]. The addition of [P$_{14,6,6,6}$][Tf$_2$N] reduces the size of the spherical balls and produces flat surface with lesser number of pores. Adding 25 wt% of [P$_{14,6,6,6}$][Tf$_2$N] produces maximum pores in prepared SPEs, while GPE has more number of pores than that. These pores were responsible for ionic conduction and reduced spherical balls forms more amorphous network which results in high ionic conductivity, as discussed in XRD and ionic conductivity studies.

3.5 Thermal studies

The thermo gravimetric and differential thermal analysis (TGDTA) was used to study the thermal stability of the prepared electrolyte samples. Generally, the pure [P$_{14,6,6,6}$][Tf$_2$N] ionic liquid has the thermal stability of 350 °C as reported by Battez et al. [29], whereas the ionic liquid incorporated polymer electrolyte has maintained the maximum thermal stability of 300 °C with 22% weight loss. The thermal stability of prepared electrolytes was measured from 32 to 900 °C having two weight loss regions. The first degradation temperature has been found nearly at 320 °C corresponding to the decomposition of the ionic liquid medium with the weight loss of 20 wt%. The complete decomposition temperature of polymer electrolyte has appeared around 500 °C showing the melting of the polymer electrolyte in nitrogen controlled atmosphere. The deep weight loss of about 60% is also noted indicating the decomposition temperature of polymer electrolyte. Among the samples studied, the electrolyte with higher ionic conductivity has maximum thermal stability of 260 °C. Compared to SPEs, the GPE has less stability around 260 °C, due to the evaporation of molecular solvents. The maximized region in Fig. 6 clearly shows the weight loss region of the individual polymer electrolytes. The remaining weight percentage may be due to the presence of residual carbon in the polymer electrolytes. A typical DTA curve for the polymer
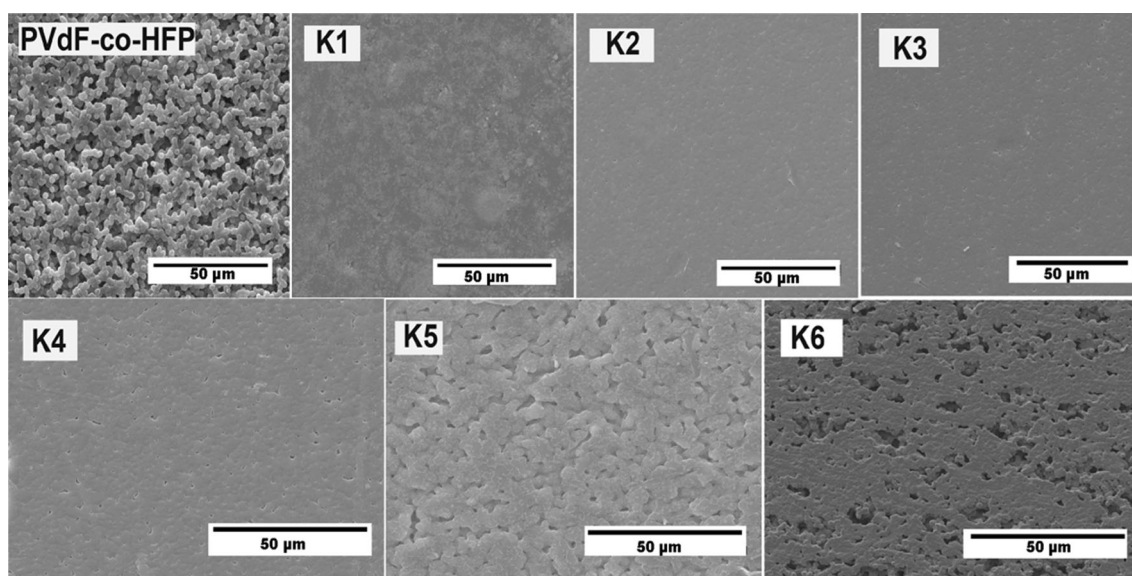
Fig. 5 SEM image of pure P(VdF-*co*-HFP), SPE K1-(95:5), K2- (90:10), K3- (85:15), K4- (80:20), K5- (75:25) of P(VdF-*co*-HFP) + [P$_{14,6,6,6}$][Tf$_2$N] and GPE K6-PVdF-*co*-HFP + [P$_{14,6,6,6}$][Tf$_2$N] (75:25) + EC + PC (60) wt% magnification of 1 K
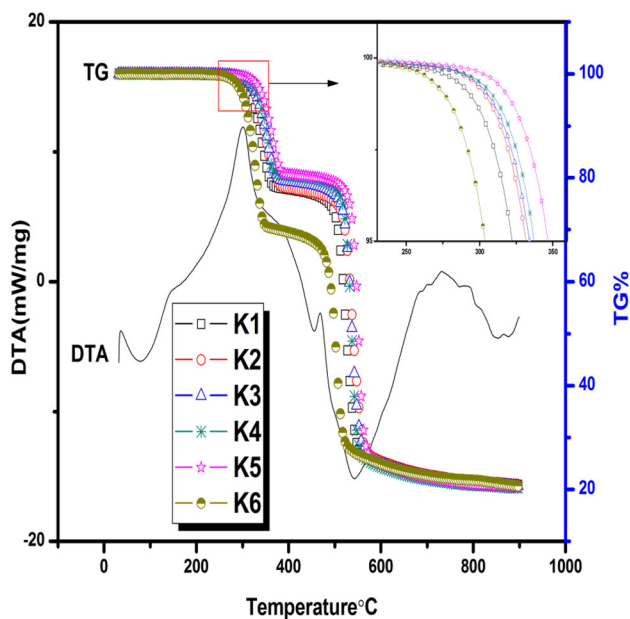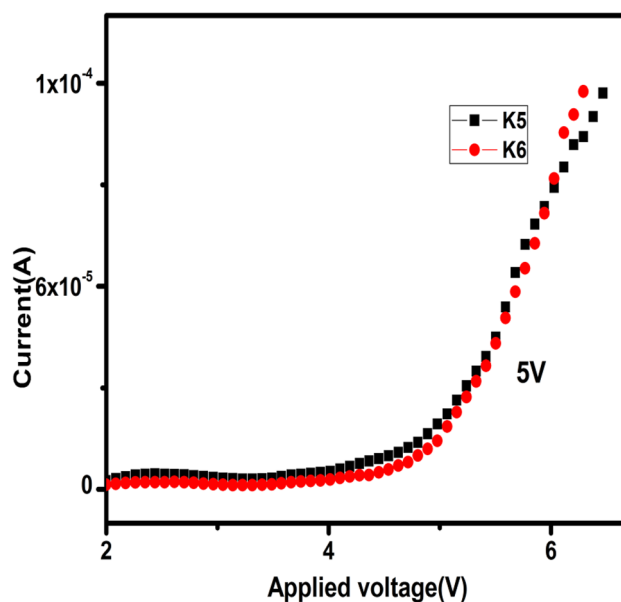
Fig. 6 TGDTA graph of SPE K1-(95:5), K2- (90:10), K3-(85:15), K4- (80:20), K5- (75:25) of P(VdF-*co*-HFP) + [P$_{14,6,6,6}$][Tf$_2$N] and GPE K6 P(VdF-*co*-HFP) + [P$_{14,6,6,6}$][Tf$_2$N] (75:25) + EC + PC (60) wt% and typical DTA plot of SPE

Fig. 7 LSV of SPE K5 P(VdF-*co*-HFP) + [P$_{14,6,6,6}$][Tf$_2$N] (75:25) and GPE K6 P(VdF-*co*-HFP) + [P$_{14,6,6,6}$][Tf$_2$N] (75:25) + EC + PC (60) wt% at a scan rate of 5 mV/s

electrolytes (SPE) has also been displayed. Corresponding exothermic curves also noted around 300 °C, 470 °C and 720 °C shows the inline behavior of the TG and DTA. The higher ionic conducting sample has been found as a suitable electrolyte for further electrochemical studies.

3.6 Linear sweep voltammetry

The linear sweep voltammetry technique (LSV) was used to find the electrochemical stability of polymer electrolyte and presented in Fig. 7. It is noted that the present polymer electrolyte samples shows no observable current through the working electrode from open circuit 4.8 V. Gradually increasing electrode potential above 4.8 V shows the electrochemical stability of polymer electrolyte. A significant electrochemical stability upto 4.8 V (K5) and 5 V (K6) were noted with a scanning rate of 5 mV/s. This stability is higher than the commercially available electrolytes for lithium batteries with the working voltage of 4.2 V. Also the electrolytes with plasticizer (GPE) have electrochemical stability slightly higher than the SPE. The anodic current is stable upto 4.8 V and after that, a sharp increase in anodic current is noted and the current that is related to the decomposition of the

polymer electrolyte. This represents the electrochemical reaction of the electrode with the polymer electrolyte [34].

3.7 Cyclic voltammetry

Cyclic voltammetry of coin cell with P(VdF-*co*-HFP) (75 wt%) + [P$_{14,6,6,6}$][Tf$_2$N] (25 wt%) and (75:25) of P(VdF-*co*-HFP): [P$_{14,6,6,6}$][Tf$_2$N] (40 wt%) + EC + PC (60 wt%) as electrolytes with LiFePO$_4$ cathode taken at room temperature for the first three consecutive cycles at a scan rate of 5 mV s^{-1} is shown in Fig. 8a, b. The first scan starts with an oxidation peak (3.42 for K5 and 3.57 for K6) followed by a reduction peak (3.2 V). The appearance of oxidation and reduction peaks suggests the strong reversible behavior of electrolyte material. Repeated scan for the consecutive cycles shows the overlapping of the curves, and this is mainly related with the reversibility. The increasing oxidation peak indicates the decompositions of the polymer electrolyte. The formation of solid electrolyte interface (SEI) on the electrode surface are identified by the decreasing the current in the second and third cycles. The SEI formation prevents further reaction of ionic liquid with lithium electrode. It is also noted that the oxidation happens within clear and high current conduction for the phosphonium-based sample. However, a feeble current
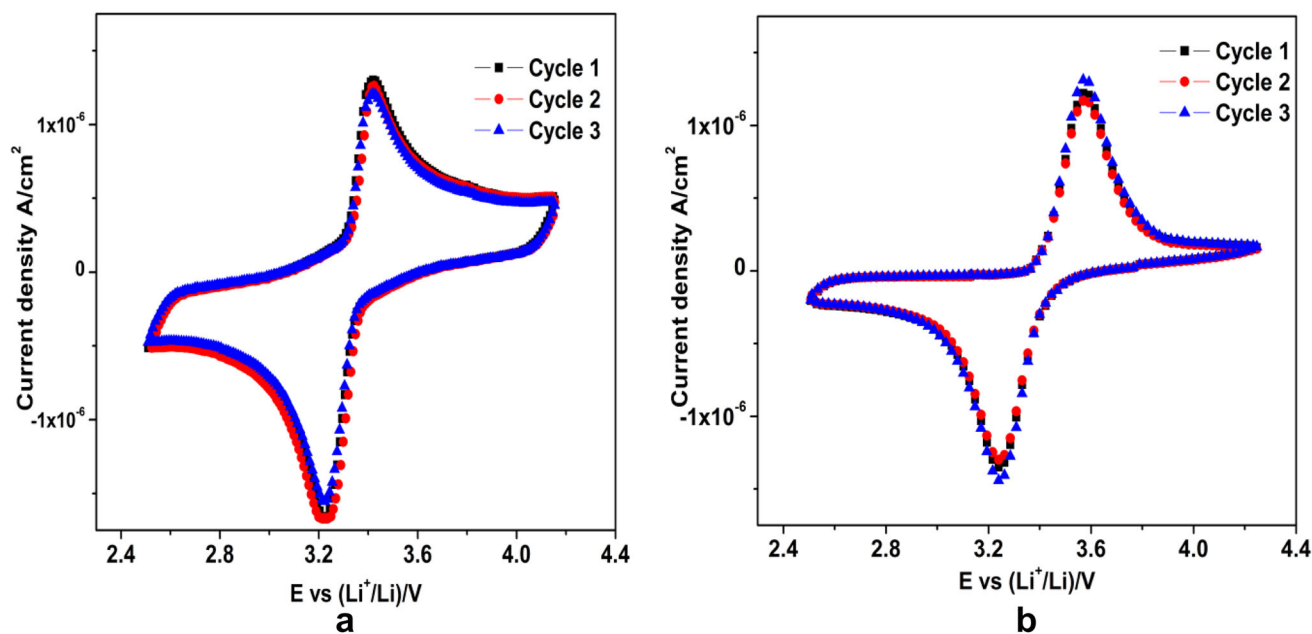
Fig. 8 Cyclic voltammetry of **a** SPE K5 P(VdF-*co*-HFP) + [P$_{14,6,6,6}$][Tf$_2$N] (75:25) and **b** GPE K6 P(VdF-*co*-HFP) + [P$_{14,6,6,6}$][Tf$_2$N] (75:25) + EC + PC (60) wt% at a scan rate of 5 mV/s

conduction was observed for sulfonium-based electrolytes which is due to the lesser corrosive nature of phosphonium IL with the electrode in the cell.
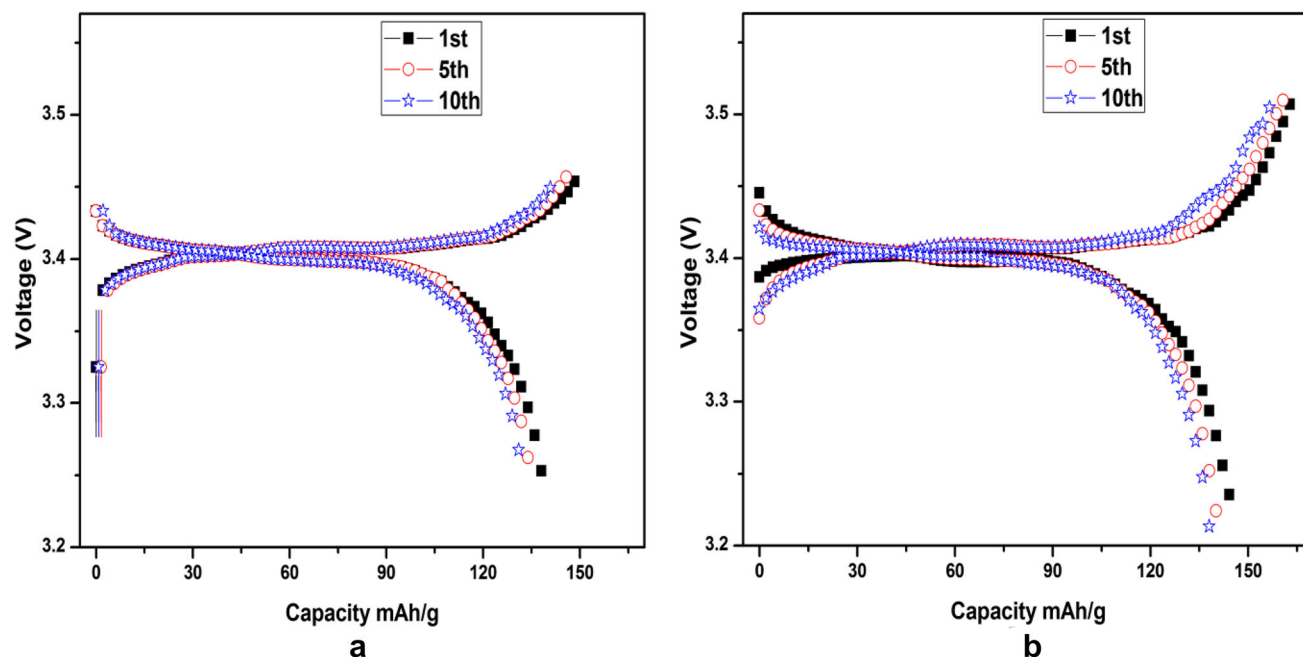
3.8 Charge discharge studies

Coin cells have been assembled with Li metal/LiFePO$_4$ electrodes containing P(VdF-*co*-HFP) (75 wt%) + [P$_{14,6,6,6}$][Tf$_2$N] (25 wt%) and (75:25) ratio of P(VdF-*co*-HFP) + [P$_{14,6,6,6}$][Tf$_2$N] (40 wt%) − EC + PC (60 wt%) electrolyte to investigate the charge/discharge performance. Figure 9a, b show the cyclic voltage profile of first, fifth and tenth cycles. A flat voltage plateau has been obtained with voltage range of 3.4 V. A columbic efficiency of above 85% has been obtained in the first cycle for both samples. The coin cell fabricated with K5 sample delivers a discharge value of about 137 mAh/g, whereas, the plasticizer embedded system delivers 146 mAh/g [36]. The discharge capacity in the multiple cycles decreases with the increase of cycle numbers. The decrease in discharge capacity is mainly due to the formation of passive layer on the cathode material. Finally, in the tenth cycle, the capacity values of charge/discharge reached to 142/131 mAh/g (K5) and 157/136 mAh/g (K6) respectively. Comparing with the previous literature reports [37–39], the present work revealed a better discharge capacity due to the phosphonium-

based ionic liquids. From the above studies, it is concluded that the plasticizer embedded system has more discharge capacity and it is suitable as electrolyte for lithium secondary batteries.

4 Conclusion

This study reports the physical and electrochemical properties of polymer electrolytes composed of phosphonium ionic liquid incorporated with P(VdF-*co*-HFP) solid and gel polymer electrolytes. All the electrolytes were characterized using XRD, FTIR, TG–DTA and SEM. It is concluded that the 75:25 wt% of P(VdF-*co*-HFP): Phosphonium IL electrolytes exhibit maximum conductivity and this drives the properties too. Also using this ratio of polymer and IL the effect of addition of plasticizer has been tested and concluded with the appreciable properties in all aspects. The addition of plasticizer would result in higher ionic conductivity and wide working voltage, however affects the thermal stability. From the experimental studies, it is observed that all the electrolytes follow Arrhenius behavior, where the best ionic conductivity of 3.40 × 10^{-4} S/cm at 303 K has been achieved for the GPE with minimal activation energy value of 0.197 eV. Samples containing maximum ionic conductivity have necessary porosity with

Fig. 9 Charge discharge profile of **a** SPE K5 P(VdF-*co*-HFP) + [P$_{14,6,6,6}$][Tf$_2$N] (75:25), **b** GPE K6 P(VdF-*co*-HFP) + [P$_{14,6,6,6}$][Tf$_2$N] (75:25) + EC + PC (60) wt% for first, fifth and tenth cycles

network structure, which is revealed by SEM images. The sample K6 is found to have thermal stability upto 260 °C with a wide electrochemical window of 5 V and discharge capacity of 146 mAh/g in lithium battery. Further, phosphonium ionic liquid-based polymer electrolyte incorporated with inorganic filler will be studied to improve the performance of composite gel polymer electrolyte.

Acknowledgements

References

1. M. Osinska, M. Walkowiak, A. Zalewska, T. Jesionowski, Study of the role of ceramic filler in composite gel electrolytes based on microporous polymer membranes. J. Membr. Sci. **326**(2), 582–588 (2009). https://doi.org/10.1016/j.memsci.2008.10.036

2. Y. Xia, T. Fujieda, K. Tatsumi, P.P. Prosini, T. Sakai, Thermal and electrochemical stability of cathode materials in solid polymer electrolyte. J. Power Sources **92**(1–2), 234–243 (2001). https://doi.org/10.1016/S0378-7753(00)00533-4

3. G. Li, Z. Li, P. Zhang, H. Zhang, Y. Wu, Research on a gel polymer electrolyte for Li-ion batteries. Pure Appl. Chem. **80**(11), 2553–2563 (2008). https://doi.org/10.1351/pac200880112553

4. C.S. Kim, S.M. Oh, Importance of donor number in determining solvating ability of polymers and transport properties in gel-type polymer electrolytes. Electrochim. Acta **45**(13), 2101–2109 (2000). https://doi.org/10.1016/S0013-4686(99)00426-0

5. F.B. Dias, L. Plomp, J.B. Veldhuis, Trends in polymer electrolytes for secondary lithium batteries. J. Power Sources **88**(2), 169–191 (2000). https://doi.org/10.1016/S0378-7753(99)00529-7

6. O.V. Bushkova, S.E. Popov, T.V. Yaroslavtseva, V.M. Zhukovsky, A.E. Nikiforov, Ion–molecular and ion–ion interactions in solvent-free polymer electrolytes based on amorphous butadiene—acrylonitrile copolymer and LiAsF6. Solid State

Ion. **178**(35–36), 1817–1830 (2008). https://doi.org/10.1016/j.ssi.2007.11.023

7. S. Ferrari, E. Quartarone, P. Mustarelli, A. Magistris, M. Fagnoni, S. Protti, C. Gerbaldi, A. Spinella, Lithium ion conducting PVdF-HFP composite gel electrolytes based on N-methoxyethyl-N-methylpyrrolidinium bis (trifluoromethanesulfonyl)-imide ionic liquid. J. Power Sources **195**(2), 559–566 (2010). https://doi.org/10.1016/j.jpowsour.2009.08.015

8. J.P. Tafur, F. Santos, A.J. Romero, Influence of the ionic liquid type on the gel polymer electrolytes properties. Membranes **5**(4), 752–771 (2015). https://doi.org/10.3390/membranes5040752

9. D. Saikia, Y.W. Chen-Yang, Y.T. Chen, Y.K. Li, S.I. Lin, Li NMR spectroscopy and ion conduction mechanism of composite gel polymer electrolyte: A comparative study with variation of salt and plasticizer with filler. Electrochim Acta **54**(4), 1218–1227 (2009). https://doi.org/10.1016/j.electacta.2008.09.001

10. S.K. Chaurasia, R.K. Singh, Crystallization behaviour of a polymeric membrane based on the polymer PVdF–HFP and the ionic liquid BMIMBF 4. RSC Adv. **4**(92), 50914–50924 (2014). https://doi.org/10.1039/C4RA07085B

11. D. Saikia, Y.W. Chen-Yang, Y.T. Chen, Y.K. Li, S.I. Lin, Investigation of ionic conductivity of composite gel polymer electrolyte membranes based on P (VDF-HFP), LiClO4 and silica aerogel for lithium ion battery. Desalination **234**(1–3), 24–32 (2008). https://doi.org/10.1016/j.desal.0000.00.000

12. L.N. Sim, S.R. Majid, A.K. Arof, Effects of 1–butyl–3–methyl imidazolium trifluoromethanesulfonate ionic liquid in poly (ethyl methacrylate)/poly (vinylidenefluoride-co-hexafluoropropylene) blend based polymer electrolyte system. Electrochim Acta **123**, 190–197 (2014). https://doi.org/10.1016/j.electacta.2014.01.017

13. T. Michot, A. Nishimoto, M. Watanabe, Electrochemical properties of polymer gel electrolytes based on poly (vinylidene fluoride) copolymer and homopolymer. Electrochim Acta **45**(8–9), 1347–1360 (2000). https://doi.org/10.1016/S0013-4686(99)00343-6

14. B.G. Soares, K. Pontes, J.A. Marins, L.F. Calheiros, S. Livi, G.M. Barra, Poly (vinylidene fluoride-co-hexafluoropropylene)/polyaniline blends assisted by phosphonium–based ionic liquid: dielectric properties and β-phase formation. Eur. Polym. J. **73**, 65–74 (2015). https://doi.org/10.1016/j.eurpolymj.2015.10.003

15. R.E. Ramírez, L.C. Torres-González, E.M. Sánchez, Electrochemical aspects of asymmetric phosphonium ionic liquids. J. Electrochem. Soc. **154**(2), 229–233 (2007). https://doi.org/10.1149/1.2404789

16. E.H. Cha, J.Y. Mun, E. Cho, T.E. Yim, Y.G. Kim, S.M. Oh, S.A. Lim, J.W. Lim, The corrosion study of al current collector in phosphonium ionic liquid as solvent for lithium ion battery. J. Korean Electrochem. Soc. **14**(3), 152–156 (2011). https://doi.org/10.5229/JKES.2011.14.3.152

17. M. Taige, D. Hilbert, T.J. Schubert, Mixtures of ionic liquids as possible electrolytes for lithium ion batteries. Int. J. Res. Phys. Chem. Chem. Phys. **226**(2), 129–139 (2012). https://doi.org/10.1524/zpch.2012.0161

18. H.L. WuTY, P.R. Chen, J.W. Liao, Ionic conductivity and transporting properties in LiTFSI-doped bis (trifluoromethanesulfonyl) imide-based ionic liquid electrolyte. Int. J. Electrochem. Sci. **8**, 2606–2624 (2013)

19. S.S. Keskar, L.A. Edye, C.M. Fellows, W.O.S. Doherty, ATR-FTIR measurement of biomass components in phosphonium ionic liquids. J. Wood Chem. Technol. **32**, 175–186 (2012). https://doi.org/10.1080/02773813.2011.631718

20. S.R. Sarda, W.N. Jadhav, A.S. Shete, K.B. Dhopte, S.M. Sadawarte, P.J. Gadge, R.P. Pawar, Phosphonium ionic liquid–catalyzed Michael addition of mercaptans to α, β-unsaturated ketones. Synth. Commun. **40**(14), 2178–2184 (2010). https://doi.org/10.1080/00397910903221050

21. J.W. Vaughan, D. Dreisinger, J. Haggins, Density, viscosity, and conductivity of tetraalkyl phosphonium ionic liquids. ECS Trans. **2**(3), 381–392 (2006). https://doi.org/10.1149/1.2196027

22. A.F. Ferreira, P.N. Simoes, A.G. Ferreira, Quaternary phosphonium-based ionic liquids: thermal stability and heat capacity of the liquid phase. J. Chem. Thermodyn. **45**(1), 16–27 (2012). https://doi.org/10.1016/j.jct.2011.08.019

23. M. Nadherna, J. Reiter, J. Moskon, R. Dominko, Lithium bis (fluorosulfonyl) imide–PYR14TFSI ionic liquid electrolyte compatible with graphite. J. Power Sources **196**(18), 7700–7706 (2011). https://doi.org/10.1016/j.jpowsour.2011.04.033

24. P.A. Thomas, B.B. Marvey, Room temperature ionic liquids as green solvent alternatives in the metathesis of oleochemical feedstocks. Molecules **21**(2), 184 (2016). https://doi.org/10.3390/molecules21020184

25. A.J. Rennie, N. Sanchez-Ramirez, R.M. Torresi, P.J. Hall, Ether-bond-containing ionic liquids as supercapacitor electrolytes. J Phys Chem Lett **4**(17), 2970–2974 (2013). https://doi.org/10.1021/jz4016553

26. R. Zhang, Y. Chen, R. Montazami, Ionic liquid-doped gel polymer electrolyte for flexible lithium-ion polymer batteries. Materials **8**(5), 2735–2748 (2015). https://doi.org/10.3390/ma8052735

27. S.K. Chaurasia, R.K. Singh, S. Chandra, Thermal stability, complexing behavior, and ionic transport of polymeric gel membranes based on polymer PVdF-HFP and ionic

liquid,[BMIM][BF4]. J. Phys. Chem. B **117**(3), 897–906 (2013). https://doi.org/10.1021/jp307694q

28. P.K. Singh, K.C. Sabin, X. Chen, Ionic liquidsolid polymer electrolyte blends for supercapacitor applications. Polym. Bull. **73**, 255–263 (2016). https://doi.org/10.1007/s00289-015-1484-3

29. M. Wang, S.A. Vail, A.E. Keirstead, M. Marquez, D. Gust, A.A. Garcia, Preparation of photochromic poly (vinylidene fluoride-co-hexafluoropropylene) fibers by electrospinning. Polymer **50**(16), 3974–3980 (2009). https://doi.org/10.1016/j.polymer.2009.06.044

30. A.H. Battez, M. Bartolome, D. Blanco, J.L. Viesca, A. Fernandez-Gonzalez, R. Gonzalez, Phosphonium cation-based ionic liquids as neat lubricants: physicochemical and tribological performance. Tribol. Int. **95**, 118–131 (2016). https://doi.org/10.1016/j.triboint.2015.11.015

31. M. Dobbelin, I. Azcune, M. Bedu, A. Ruiz de Luzuriaga, A. Genua, V. Jovanovski, G. Cabanero, I. Odriozola, Synthesis of pyrrolidinium-based poly (ionic liquid) electrolytes with poly (ethylene glycol) side chains. Chem. Mater. **24**(9), 1583–1590 (2012). https://doi.org/10.1021/cm203790z

32. A.R. Polu, D.K. Kim, H.W. Rhee, Poly (ethylene oxide)-lithium difluoro (oxalato) borate new solid polymer electrolytes: ion–polymer interaction, structural, thermal, and ionic conductivity studies. Ionics **21**(10), 2771–2780 (2015). https://doi.org/10.1007/s11581-015-1474-1483

33. F. Deng, X. Wang, D. He, J. Hu, C. Gong, Y.S. Ye, X. Xie, Z. Xue, Microporous polymer electrolyte based on PVDF/PEO star polymer blends for lithium ion batteries. J. Membr. Sci. **491**, 82–89 (2015). https://doi.org/10.1016/j.memsci.2015.05.021

34. M. Ravi, S. Song, J. Wang, T. Wang, R. Nadimicherla, Ionic liquid incorporated biodegradable gel polymer electrolyte for lithium ion battery applications. J. Mater. Sci.: Mater. Electron. **27**(2), 1370–1377 (2016). https://doi.org/10.1007/s10854-015-3899-x

35. J.H. Shin, W.A. Henderson, C. Tizzani, S. Passerini, S.S. Jeong, K.W. Kim, Characterization of solvent-free polymer electrolytes consisting of ternary PEO–LiTFSI–PYR14 TFSI. J. Electrochem. Soc. **153**(9), A1649-1654 (2006). https://doi.org/10.1149/1.2211928

36. K. Tsunashima, F. Yonekawa, M. Kikuchi, M. Sugiya, Tributylmethylphosphonium Bis (trifluoromethylsulfonyl) amide as an effective electrolyte additive for lithium secondary batteries. J. Electrochem. Soc. **157**(11), A1274-1278 (2010). https://doi.org/10.1149/1.3490662

37. K. Xu, Nonaqueous liquid electrolytes for lithium-based rechargeable batteries. Chem. Rev. **104**(10), 4303–4418 (2004). https://doi.org/10.1021/cr030203g

38. S. Seki, Y. Ohno, Y. Mita, N. Serizawa, K. Takei, H. Miyashiro, Imidazolium-based room-temperature ionic liquid for lithium secondary batteries: relationships between lithium salt concentration and battery performance characteristics. ECS Electrochem. Lett. **1**(6), A77 (2012). https://doi.org/10.1149/2.003206eel

39. A. Swiderska-Mocek, Electrolyte based on 1-ethyl-3-vinylimidazolium bis (trifluoromethanesulphonyl) imide for Li-ion batteries. Electrochim Acta **132**, 504–511 (2014). https://doi.org/10.1016/j.electacta.2014.03.185

Publisher's Note Springer Nature remains neutral with regard to jurisdictional claims in published maps and institutional affiliations.